AIP | Journal of Applied Physics

# Color of TiN and ZrN from first-principles calculations

Jinwoong Kim, Seung-Hoon Jhi, and Kwang Ryeol Lee

Citation: J. Appl. Phys. **110**, 083501 (2011); doi: 10.1063/1.3650264
View online: http://dx.doi.org/10.1063/1.3650264
View Table of Contents: http://jap.aip.org/resource/1/JAPIAU/v110/i8
Published by the American Institute of Physics.

## Related Articles

Spectroscopic characteristics of Dy3+ doped Y3Al5O12 transparent ceramics
J. Appl. Phys. 110, 083120 (2011)

Electron spin state tomography with coherent Kerr effect
Appl. Phys. Lett. 99, 173108 (2011)

Polarization of conducting nanoparticles
J. Appl. Phys. 110, 084314 (2011)

Index of refraction of shock-released materials
J. Appl. Phys. 110, 083509 (2011)

Composition dependence of dispersion and bandgap properties in PZN-xPT single crystals
J. Appl. Phys. 110, 083513 (2011)

## Additional information on J. Appl. Phys.

Journal Homepage: http://jap.aip.org/
Journal Information: http://jap.aip.org/about/about_the_journal
Top downloads: http://jap.aip.org/features/most_downloaded
Information for Authors: http://jap.aip.org/authors

ADVERTISEMENT

AIP Advances
Submit Now
Explore AIP's new open-access journal
• Article-level metrics now available
• Join the conversation! Rate & comment on articles

Downloaded 01 Nov 2011 to 161.122.23.125. Redistribution subject to AIP license or copyright; see http://jap.aip.org/about/rights_and_permissions

# Color of TiN and ZrN from first-principles calculations

Jinwoong Kim,[1] Seung-Hoon Jhi,[1,2,a)] and Kwang Ryeol Lee[3]
[1]*Department of Physics, Pohang University of Science and Technology, Pohang 790-784, South Korea*
[2]*Division of Advanced Materials Science, Pohang University of Science and Technology, Pohang 790-784, South Korea*
[3]*Computational Science Center, Korea Institute of Science and Technology, Seoul 136-791, South Korea*

(Received 5 July 2011; accepted 31 August 2011; published online 17 October 2011)

The optical properties, especially the colors, of transition metal nitrides (TiN and ZrN) are studied using first-principles method. Full *ab-initio* procedure of color-prediction including plasma frequency is presented. The dielectric functions and reflectivity of the compounds are calculated including both intraband and interband transitions. The color of the compounds is then produced by calculating the red-green-blue color codes through the convolution of color matching functions and the calculated reflectivity. Calculated colors and screened plasma frequency for the materials are in good agreement with measurement. The color variation due to chemical doping is also studied within the rigid band approximation. © *2011 American Institute of Physics*. [doi:10.1063/1.3650264]

## I. INTRODUCTION

Transition metal nitrides such as TiN and ZrN are widely used as coating materials for machine parts and as cutting tools due to their high hardness and strong resistivity against abrasion. Additionally, they have intrinsic gold-like metallic colors,[1–5] which are tunable by adding impurities while maintaining good mechanical properties. This extra merit extends the area of practical application from industrial machineries to fancy daily goods, and the color adjustment in coating is actively sought. Normally color variation in these materials has been attempted in empirical basis. It was found that defects or substitutional doping change their colors to black,[6] gray,[7] red,[2,3] violet[8] or even to dark blue.[2] There have been several studies[4,5] to explain the color variation from the alteration in plasma frequency or absorption spectrum, which corresponds to intraband transition or interband transition, respectively. While mechanical and electrical properties of the materials have been extensively studied from first-principles calculations,[9–12] predicting the color by calculations has not been given a full attention because the color has generally been considered to be a quality resulting from complex optical and visual processes. Recently Xue *et al*. studied the color variation of $Na_xWO_3$ with *ab-initio* calculations[13] while employing experimental values of plasma frequency. Here, we present a procedure to calculate the colors of transition metal compounds based on full *ab-initio* calculations including plasma frequency. The color of transition metal nitrides is produced from first-principles calculations, and the contribution of specific transitions is investigated. The effect of C or O impurities is also studied within the rigid band approximation.

## II. METHODS

Two most responsible processes for scattering of light in the visible range are the intraband and interband transitions of electrons.[14,15] Such scattering processes are characterized by the dielectric function of the material.[15,16] The intraband transition is the plasma resonance absorption process by unbound electrons that have a collective oscillation mode at the Fermi surface with the plasma frequency. Therefore, if the frequency of an incident light is similar to the plasma frequency of a material, the light would be absorbed through resonance. Incident lights with frequency less (higher) than the plasma frequency are 100% reflected (transmitted). This is a well-known explanation of high-glossy and colorless feature of metals. A critical parameter that characterizes colors is thus the plasma frequency[15]

$$\omega_p^2 = \frac{e^2}{8\pi^3\hbar^2\varepsilon_0}\sum_n \int \left(\frac{\partial E_{n\mathbf{k}}}{\partial \mathbf{k}}\right)^2 \delta(E_{n\mathbf{k}} - E_F)\mathrm{d}^3\mathbf{k}, \quad (1)$$

where $E_{n\mathbf{k}}$ is the energy eigen-value of the Bloch state at $n$th band at $k$ point and $E_F$ is the Fermi level.

The dielectric function due to the intraband transition can be calculated using Drude model with given plasma frequency,[15,17]

$$\varepsilon^{\mathrm{intra}}(\omega) = 1 - \frac{\omega_p^2}{\omega(\omega + i\gamma)}, \quad (2)$$

where $\gamma(=\hbar/\tau)$ is the inverse of relaxation time $\tau$ of the unbound electrons. This equation shows that the real part of the dielectric function will be very small near the plasma frequency. The location of absorption peaks can be found from the zeros of real part dielectric functions. This scheme is used to determine the screened plasma frequency as described below.

The absorption spectrum from interband transitions is computed from electronic band structures. One crucial role of the interband transition is the screening of unbound electrons, which reduces the plasma frequency. When the plasma frequency is shifted into a visible-light range (~1.7–3.1 eV) by the screening, metals have certain metallic colors as in the case of copper and gold, in which low energy (red-yellow range) photons are reflected while high energy (blue-violet range) photons are absorbed or transmitted. The imaginary part of the dielectric function by interband transition is calculated by the following formula:[14,15]

a)Electronic mail: jhish@postech.ac.kr.

 © 2011 American Institute of Physics

Downloaded 01 Nov 2011 to 161.122.23.125. Redistribution subject to AIP license or copyright; see http://jap.aip.org/about/rights_and_permissions

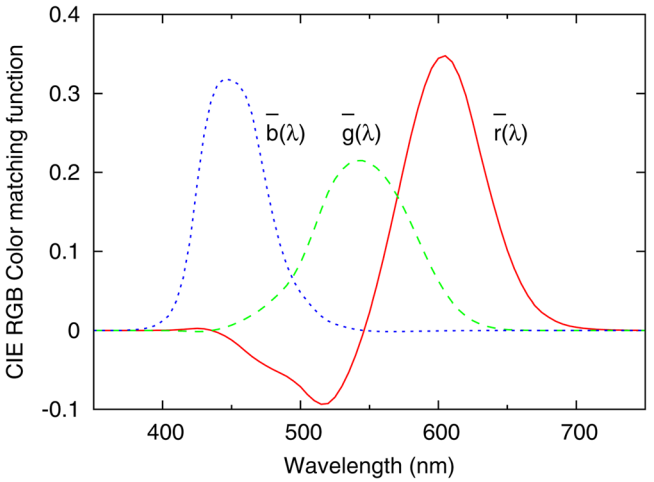


FIG. 1. (Color online) CIE RGB color matching functions used in this study; red (solid line), green (dashed line), and blue (dotted line) fractions in monochromatic light as announced by CIE in 1931.[18,19]

$$\varepsilon_2^{\text{inter}}(\omega) = \frac{e^2\hbar^2}{8\pi^3\varepsilon_0 m_0^2}\sum_{m>n}\int \frac{\{f(E_{n\mathbf{k}}) - f(E_{m\mathbf{k}})\} \times |\langle m\mathbf{k}|\hat{p}|n\mathbf{k}\rangle|^2}{E_{m\mathbf{k},n\mathbf{k}}(E_{m\mathbf{k},n\mathbf{k}}^2 - \hbar^2\omega^2)} d^3\mathbf{k}, \tag{3}$$

where $f$ is the Fermi-Dirac distribution, $\hat{p}$ is the momentum operator, and $E_{m\mathbf{k},n\mathbf{k}} = E_{m\mathbf{k}} - E_{n\mathbf{k}}$ (the energy difference between single-particle Bloch states). The real part $\varepsilon_1^{\text{inter}}(\omega)$ is then obtained from the Kramers-Kronig relation.

The total dielectric function is the sum of those by intraband and interband transitions, $\varepsilon(\omega) = \varepsilon^{\text{intra}}(\omega) + \varepsilon^{\text{inter}}(\omega)$.

Optical properties are readily obtained from the dielectric function; the reflectivity for unpolarized normal-incident light is given by $R(\omega) = \left|(1 - \sqrt{\varepsilon(\omega)})/(1 + \sqrt{\varepsilon(\omega)})\right|^2$ and the absorption (energy loss) spectrum is $L(\omega) = -\text{Im}\,[1/\varepsilon(\omega)] = \varepsilon_2/(\varepsilon_1^2 + \varepsilon_2^2)$ (Ref. 16). The absorption spectrum has peaks at the frequencies where the real part dielectric function becomes zero. Therefore, the screened plasma frequency, $\omega_p'$, is determined from $\varepsilon_1(\omega_p') = 0$ or from the position of absorption maxima.

The Commission Internationale de l'Eclairage (CIE) developed color-matching functions, $\bar{r}(\lambda)$, $\bar{g}(\lambda)$, $\bar{b}(\lambda)$ that convert the spectral power distribution $\text{I}(\lambda)$ into red-green-blue (RGB) codes[18] as expressed by

$$\begin{aligned} R &= \int_0^\infty \bar{\text{r}}(\lambda)\text{I}(\lambda)\text{d}\lambda, \\ G &= \int_0^\infty \bar{\text{g}}(\lambda)\text{I}(\lambda)\text{d}\lambda, \\ B &= \int_0^\infty \bar{\text{b}}(\lambda)\text{I}(\lambda)\text{d}\lambda. \end{aligned} \tag{4}$$

If we assume a uniform intensity ($I_0$) of incident light over the wavelength of interest, the reflected light will have the same intensity distribution as the reflectivity, $I(\lambda) = R(\lambda) \times I_0$. The reflected light is then decomposed into red, green, and blue components by using Eq. (4). Therefore, the color of a material can be calculated from first-principles in the following steps; calculate first the dielectric function from interband and intraband transitions, second the reflectivity, and last RGB codes using color matching functions. Calculated RGB color codes can also be converted to CIE L*a*b* color space,[19] which is the standard representation of colors in industry. In L*a*b* color space, the difference of two colors is defined as a distance between two color coordinates (L*, a*, b*), where L*, a*, and b* represent brightness, red-greenness and yellow-blueness, respectively.

First-principle calculations were carried out using density functional theory (DFT) as implemented in Vienna *ab-initio* simulation package (VASP).[20] Projector augmented wave-function (PAW) type pseudopotentials are used for the ionic potentials.[21,22] The cut-off energy of the plane wave basis set was chosen to be 400 eV, and the exchange-correlation functional was treated within Perdew-Burke-Ernzerhof type[23] generalized gradient approximation. Brillouin zone sampling was done using Monkhorst-Pack[24] with $20 \times 20 \times 20$ grid. For ZrN case, we mixed dielectric functions obtained with Monkhorst-Pack grid (770 k-points in total) and Γ point-included grid (256 k-points in total) to properly take into account the low energy interband transitions. The mixing ratio was 75% of Monkhorst-Pack sampling and 25% of Γ point-included sampling. We employed the method presented in Ref. 25 to calculate the dielectric function from interband transition. The plasma frequency was calculated using Eq. (1) and the tetrahedron method[26] for k-point integration.

## III. RESULTS AND DISCUSSION

TiN and ZrN have NaCl structure, and our calculated lattice constants are 4.255 Å and 4.610 Å, respectively, in good agreement with experiment.[27] Calculated bulk modulus (291 GPa for TiN and 262 GPa for ZrN) is also consistent with the results in previous studies.[9,10] Figure 2 shows the calculated band structures of TiN and ZrN. Partially filled *d*-bands are observed near the Fermi level ($E_f$). While the selection rule forbids the *d*-*d* transitions, the hybridization between transition metal *d* and nitrogen *p* orbitals allows the optical transitions between the *d*-bands near $E_f$. Along the Brillouin zone edges (X-W-L and K-W, particularly), strong interband transitions occur with transition energies of 5–8 eV and 6–9 eV for TiN and ZrN, respectively. Such transitions

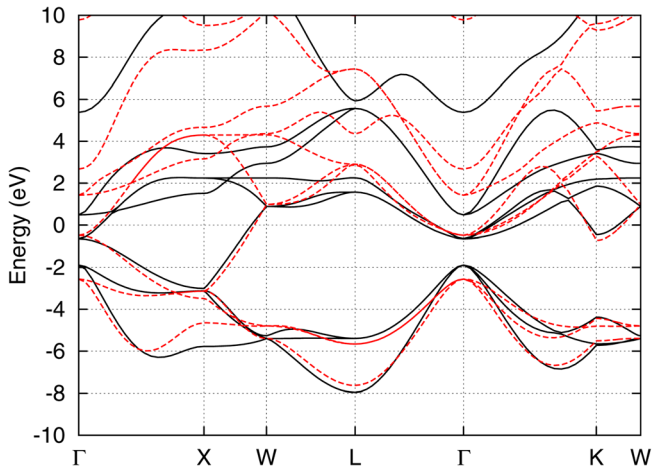


FIG. 2. (Color online) Calculated band structures of TiN (black solid line) and ZrN (red dashed line). The Fermi level is set at 0 eV.

Downloaded 01 Nov 2011 to 161.122.23.125. Redistribution subject to AIP license or copyright; see http://jap.aip.org/about/rights_and_permissions

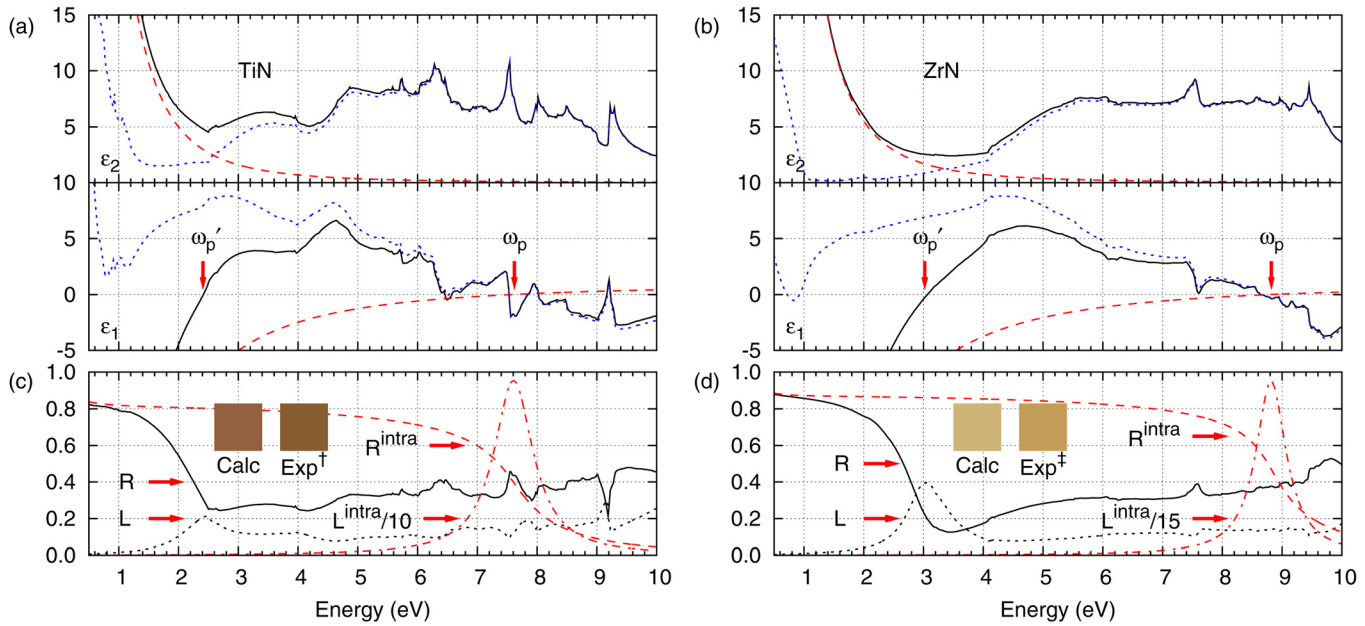


FIG. 3. (Color online) Calculated dielectric functions of (a) TiN and (b) ZrN. Upper panel, imaginary part; lower panel, real part. Contribution of intraband (red dashed line) and interband (blue dotted line) transitions to the total dielectric function (solid line) was also plotted separately. The bare plasma frequency, $\omega_P$ (7.62 eV for TiN; 8.82 eV for ZrN) is shifted to the screened plasma frequency, $\omega_p'$ (2.41 eV for TiN; 3.06 eV for ZrN) when the effect of interband transition ($\epsilon_1^{inter}(\omega)$) is added. Calculated reflectivity (R, solid line) and absorption (L, dotted line) spectra are shown in (c) for TiN and (d) for ZrN. Again, the contribution from the intraband transition is separately plotted ($R^{intra}$, red dashed line; $L^{intra}$, red dotted-dashed line). Computer-generated colors from our calculations and experiment (†Ref. 2 for TiN and ‡Ref. 3 for ZrN) are drawn for comparison as inset.

produce hills in $\varepsilon_2^{inter}$ in the corresponding energy range as shown in Figs. 3(a) and 3(b) (blue dotted line). Three parabolic bands near the Γ point contribute to low energy transitions (<1 eV). In Fig. 3, $\varepsilon_2^{inter}$ of TiN and ZrN has a broad and large peak below 1 eV due to such low energy transitions.

The plasma frequencies obtained from Eq. (1) are 7.62 eV and 8.82 eV for TiN and ZrN, respectively, which are larger than measured values by about 1 eV (Table I). This discrepancy may originate from fitting procedure of experimental data; the plasma frequency in experiment is usually obtained by fitting measured dielectric functions to Drude model [Eq. (2)] at low energy range while ignoring interband transitions. However, there are significant contributions from interband transitions in below 1 eV. For the inversed relaxation time ($\gamma$) of unbound electrons, we used measured values of 0.8 eV and 0.62 eV for TiN and ZrN, respectively.[1] With given this plasma frequency and relaxation time, the dielectric function of intraband transition was calculated using Eq. (2), and Figs. 3(a) and 3(b) show our calculated results (red dashed line). The reflectivity and absorption spectra of the intraband transition are also shown in Figs. 3(c) and 3(d). The position of absorption peak and

TABLE I. Calculated bare ($\omega_P$) and screened ($\omega_p'$) plasma frequencies for TiN and ZrN. The screened plasma frequency determined at absorption maxima is given in the parenthesis with *. The inverse of relaxation time ($\gamma$) in our calculations, which is adopted from Ref. 1, is also given. Experimental values are given for comparison. Calculated and measured CIE color space coordinates (L*a*b*) for the two compounds are shown.

| | TiN | | | ZrN | | |
|---|---|---|---|---|---|---|
| | $\omega_p$ (eV) | $\omega_p'$(eV) CIE L*a*b* color space | $\gamma$ (eV) | $\omega_p$ (eV) | $\omega_p'$ (eV) CIE L*a*b* color space | $\gamma$ (eV) |
| Calculated | 7.62 | 2.41 (2.47)* (70.7, 10.6, 23.2) | 0.8 | 8.82 | 3.06 (3.08)* (87.1, −2.95, 26.1) | 0.62 |
| Experimental | 6.9-7[a] | 2.8[a] | 0.6-0.8[a] | 7.3-7.8[a] | 3.1[a] | 0.52-0.62[a] |
| | 6.9[b] | 2.5[b] | 0.08[b] | 7.35[e] | 3.08[e] | 0.59[e] |
| | 6.29[c] | 2.52[c] | 0.3[c] | 7.17[f] | ~3[f] | 0.35[f] |
| | 7.3[d] | 2.5[d] | 0.4-0.7[d] | | | |
| | | (69.2 ± 3.5, 6.0 ± 1.6, 30.9 ± 1.2)[g] | | | (84.2, −0.7, 32.1)[h] | |

[a]Reference 1.
[b]Reference 5.
[c]Reference 28.
[d]Reference 29.
[e]Reference 30.
[f]Reference 31.
[g]Reference 2.
[h]Reference 3.

Downloaded 01 Nov 2011 to 161.122.23.125. Redistribution subject to AIP license or copyright; see http://jap.aip.org/about/rights_and_permissions

the reflectivity edge are located at the plasma frequency $\omega_P$ for which $\varepsilon_1^{\text{intra}}(\omega_P) = 0$. Including the screening of bound electrons, the screened plasma frequency $\omega_p'$ was obtained from $\varepsilon_1(\omega_p') = 0$. Figure 3 shows that the plasma frequency that includes only the contribution from the intraband transition is displaced to the screened plasma frequency when the interband transition is considered. In our calculations, the screened plasma frequencies are obtained to be 2.41 eV for TiN and 3.06 eV for ZrN. These screened plasma frequencies lie in the visible spectrum range that corresponds to the metallic colors. Our calculated screened plasma frequencies are close to experimental values of 2.5–2.8 eV (Refs. 1, 5, 28, and 29) and 3.08–3.1 eV (Refs. 1 and 30) for TiN and ZrN, respectively. The computer-generated colors using the RGB color codes from spectral decomposition are shown in the inset and look gold-like as observed in these materials. The reflectivity of ZrN below the absorption peak is larger by about 10% than that of TiN. This indicates that ZrN is brighter than TiN, which is consistent with observations.[2,3] The CIE L*a*b* color codes[19] are also close to the measured values (Table I).

Next, we studied the effect of doping on color variation within the rigid band approximation as it is known that transition metal carbides and nitrides exhibit very similar electronic structure except the Fermi level position.[11,12] For instance, carbon or oxygen substitution for nitrogen can be treated within the approximation, removing or adding one electron per each atomic substitution. Other defect structures such as interstitials or vacancies, which may be created by oxygen doping, are not considered here. Most apparent effect of doping is, of course, a change of plasma frequency which is directly related to the electron density. Calculated plasma frequency is plotted with respect to the doping level in Fig. 4(a). Because of the parabolic bands at Γ point, plasma frequency increases (decreases) by *n*-doping (*p*-doping). As mentioned above, calculated plasma frequencies are overestimated from experimental values, but their tendency at varying doping level is consistent with experiment.[5,28]

Another effect of the doping is the shift of the Fermi level, which affects the interband transitions, especially at low energy range. Calculated Fermi level shift and corresponding change of interband transition are shown in Figs. 4(a) and 4(b). Electron doping shifts up the Fermi level that lies in the parabolic bands (conduction bands) at Γ point, and the area of the Fermi surface is increased, which leads to an enhancement of interband transitions at low energies. This enhancement in the transition peak again increases the screened plasma frequency because the transition peak lowers the real part of the dielectric function in 1-3 eV as shown in Fig. 4(b). The color variation of TiN is accelerated by both transitions. Figure 5 shows the calculated reflectivity and corresponding colors of doped TiN. The hole doping (substitution of C for N) makes TiN darker due to the decrease of electron density and thus the plasma frequency. When the Fermi level is lowered below the bottom of the parabolic bands (conduction bands) at Γ point by hole doping, the low-energy interband transition vanishes (imaginary part in $\lesssim$1.2 eV) as shown in Fig. 4(b). In such cases, the screened plasma frequency and the absorption peak shift to

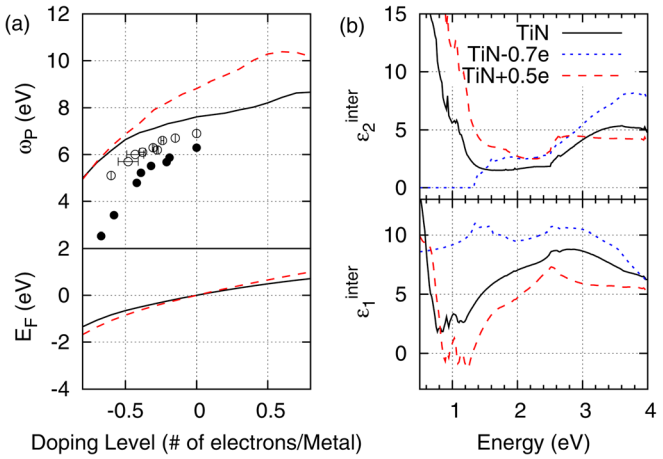


FIG. 4. (Color online) (a) Calculated plasma frequencies (upper panel) and the Fermi level shift (lower panel) of TiN (black solid line) and ZrN (red dashed line) upon substitutional doping within the rigid band approximation. Experimental data for $TiC_xN_y$ with $x + y \approx 1$ are also plotted with empty[5] and filled[28] circles. The doping level is given in unit of electron per unit formula. (b) Imaginary (upper panel) and real part (lower panel) of dielectric function due to interband transition of TiN for three different carrier densities (solid line, neutral; dashed line, +0.5 electron/formula unit; dotted line, −0.7 electron/formula unit) as controlled by substitutional doping of non-metal atoms.

energy ranges as low as infrared and the color of the compound turns dark blue (Fig. 5).

The variation in stoichiometry of TiN and ZrN due to nitrogen interstitial or vacancy defect is known to affect their color significantly. Interstitial nitrogen will make the color darker because it takes electrons from neighboring metal atoms as like hole-doping. In the case of vacancy defects, *d* electrons of the transition metal are released back to neighboring metal atoms and the materials become brighter as like electron doping. Niyomsoan *et al.*[4] measured the color of ZrN and found that it changes drastically as N/Zr ratio is

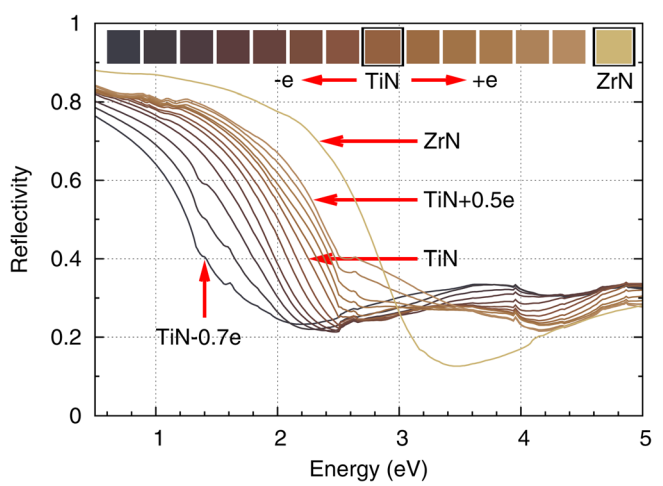


FIG. 5. (Color online) Calculated reflectivity of TiN upon electron doping. The doping level is from −0.7 to +0.5 electron per formula unit (TiN) with an increment of 0.1 electron per formula unit. The plasma frequency and the Fermi level were obtained by using the rigid band model. Color variation for corresponding reflectivity is shown in the boxes at the top. We observe that electron-poor TiN becomes darker whereas electron-rich TiN becomes brighter and more yellowish. The reflectivity and color of ZrN is also shown.

Downloaded 01 Nov 2011 to 161.122.23.125. Redistribution subject to AIP license or copyright; see http://jap.aip.org/about/rights_and_permissions

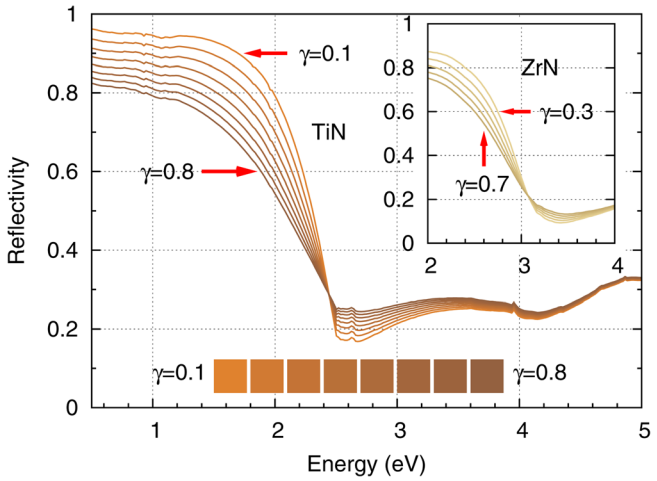


FIG. 6. (Color online) Reflectivity of TiN (also ZrN in the inset) with respect to inverse relaxation time $\gamma$ (eV). Corresponding color change is shown in the boxes in the bottom. When $\gamma$ is changed, the color looks almost the same but the chroma does change significantly.

varied, whereas the change in color of TiN is relatively unnoticeable. This different behavior of ZrN and TiN in color upon the stoichiometry is due to a more sensitive response of ZrN in the plasma frequency and Fermi level to doping compared to TiN according to our calculations [Fig. 4(a)]. Substitution of O for N is expected to produce a brighter color as it is the electron doping, but oxygen-doped TiN has a darker color in measurement.[2] This was attributed to non-uniform stoichiometry of the samples and to the interstitial oxygen defects. For later case, oxygen acts as electron accepter to make TiN hole-rich that has a dark blue color.[2]

In this study, the inverse relaxation time ($\gamma$) of electrons is the only parameter adopted from experiment. Here, we investigated the dependence of color variation on $\gamma$. We calculated the reflectivity and then the color as the parameter $\gamma$ is changed. Calculated results are presented in Fig. 6. As $\gamma$ is increased, the reflectivity is reduced (enhanced) in the frequency range lower (higher) than the screened plasma frequency and the overall brightness is diminished. This indicates that the metals will become darker as the scattering is enhanced by impurities or at elevated temperatures.[30] On the other hand, the reflectivity edge does not move at all when $\gamma$ is changed, which is due to the insensitivity of the screened plasma frequency to the relaxation time. The overall effect of the variation in $\gamma$ is thus to change the chroma rather than the hue of the compounds.

## IV. SUMMARY

We presented the full *ab-initio* procedure to calculate the color of transition-metal nitrides including both interband and intraband transitions. The only parameter undetermined was the relaxation time, which was though shown to little affect the screened plasma frequency. It was shown that computer-generated colors from calculated color codes are very close to those observed. The variation of colors of transition metal nitrides was also studied upon substitutional doping within the rigid band approximation. The electron pockets near Γ point play an important role for optical transitions and in controlling the color. The procedure of calculating colors from first-principles presented in this study can be applied to other materials and will provide efficient tools for designing materials with various colors.

## ACKNOWLEDGMENTS

This work was supported by the National Research Foundation of Korea funded by the Ministry of Education, Science and Technology (WCU program No. R31-2008-000-10059). K.R.L. was supported by Korea Institute of Science and Technology Core Capability Enhancement Program (2E22200).

[1]A. Schlegel, P. Wachter, J. J. Nickl, and H. Lingg, J. Phys. C **10**, 4889 (1977).
[2]F. Vaz, P. Cerqueira, L. Rebouta, S. M. C. Nascimento, E. Alves, P. Goudeau, and J. E. Riviere, Surf. Coat. Technol. **174**, 197 (2003).
[3]P. Carvalho, F. Vaz, L. Rebouta, L. Cunha, C. J. Tavares, C. Moura, E. Alves, A. Cavaleiro, P. Goudeau, E. Le Bourhis, J. P. Riviere, J. F. Pierson, and O. Banakh, J. Appl. Phys. **98**, 023715 (2005).
[4]S. Niyomsoan, W. Grant, D. L. Olson, and B. Mishra, Thin Solid Films **415**, 187 (2002).
[5]G. G. Fuentes, E. Elizalde, and J. M. Sanz, J. Appl. Phys. **90**, 2737 (2001).
[6]J. M. Chappe, F. Vaz, L. Cunha, C. Moura, M. C. M. De Lucas, L. Imhoff, S. Bourgeois, and J. F. Pierson, Surf. Coat. Technol. **203**, 804 (2008).
[7]J. F. Pierson, E. Tomasella, and Ph. Bauer, Thin Solid Films **408**, 26 (2002).
[8]M. Fenker, M. Balzer, H. Kappl, and O. Banakh, Surf. Coat. Technol. **200**, 227 (2005).
[9]V. P. Zhukov, V. A. Gubanov, O. Jepsen, N. E. Christensen, and O. K. Andersen, J. Phys. Chem. Solids **49**, 841 (1988).
[10]L. A. Salguero, L. Mancera, J. A. Rodríguez, and N. Takeuchi, Phys. Status Solidi (B) **243**, 1808 (2006).
[11]S.-H. Jhi, J. Ihm, S. G. Louie, and M. L. Cohen, Nature **399**, 132 (1999).
[12]S.-H. Jhi and J. Ihm, Phys. Rev. B **56**, 13826 (1997).
[13]Y. Xue, Y. Zhang, and P. Zhang, Phys. Rev. B **79**, 205113 (2009).
[14]H. Ehrenreich and M. H. Cohen, Phys. Rev. **115**, 786 (1959).
[15]T. G. Pedersen, P. Modak, K. Pedersen, N. E. Christensen, M. M. Kjeldsen, and A. N. Larsen, J. Phys. Condens. Matter. **21**, 115502 (2009).
[16]M. Fox, *Optical Properties of Solids* (Oxford University Press, New York, 2001).
[17]H. Ehrenreich and H. R. Philipp, Phys. Rev. **128**, 1622 (1962).
[18]T. Smith and J. Guild, Trans. Opt. Soc., London **33**, 73 (1931).
[19]Colorimetry, 2nd ed., CIE Publication No. 15.2, Central Bureau of the CIE, Vienna, Austria (1986).
[20]G. Kresse and J. Furthmüller, Phys. Rev. B **54**, 11169 (1996).
[21]P. E. Blöchl, Phys. Rev. B **50**, 17953 (1994).
[22]G. Kresse and D. Joubert, Phys. Rev. B **59**, 1758 (1999).
[23]J. P. Perdew, K. Burke, and M. Ernzerhof, Phys. Rev. Lett. **77**, 3865 (1996).
[24]H. J. Monkhorst and J. D. Pack, Phys. Rev. B **13**, 5188 (1976).
[25]B. Adolph, J. Furthmüller, and F. Bechstedt, Phys. Rev. B **63**, 125108 (2001).
[26]G. Lehmann and M. Taut, Phys. Status Solidi (B) **54**, 469 (1972).
[27]R. W. G. Wyckoff, *Crystal Structures*, 2nd ed. (Interscience Publishers, New York, 1963), p. 467.
[28]B. Karlsson, J.-E. Sundgren, and B.-O. Johansson, Thin Solid Films **87**, 181 (1982).
[29]E. Valkonen, C.-G. Ribbing, and J.-E. Sundgren, Appl. Opt. **25**, 3624 (1986).
[30]J. C. Francois, J. Casset, G. Chassaing, P. Gravier, and M. Sigrist, J. Appl. Phys. **58**, 3841 (1985).
[31]B. Karlsson, R. P. Shimshock, B. O. Seraphin, and J. C. Haygarth, Phys. Scr. **25**, 775 (1982).

Downloaded 01 Nov 2011 to 161.122.23.125. Redistribution subject to AIP license or copyright; see http://jap.aip.org/about/rights_and_permissions